Quadratic Rough Heston: SPX, VIX and the SSR

Jim Gatheral
(Joint work with Florian Bourgey)

Baruch COLLEGE
WEISSMAN SCHOOL OF ARTS AND SCIENCES
Master of Financial Engineering

Columbia-NYU Financial Engineering Colloquium
NYU Tandon School of Engineering
February 5, 2026

Outline of this talk

- The skew-stickiness ratio (SSR)
- The quadratic rough Heston (QRH) model
- Simulating SPX and VIX under QRH.
- The SSR under quadratic rough Heston
- Unreasonably good fit quality
- Why does QRH fit so well?

Implied volatility

According to the definition of implied volatility $\sigma_{\text{BS}}(k, T)$, the market price of an option is given by

$$C(S, K, T) = C_{\text{BS}}(S, K, T, \sigma_{\text{BS}}(k, T))$$

where C_{BS} denotes the Black-Scholes formula and $k = \log K/S$ is the log-strike.

Updating European option prices

Market makers, when updating option prices using the Black-Scholes formula, typically consider two effects:

- The explicit spot effect

$$\frac{\partial C}{\partial S}\,\delta S$$

and

- The change in implied volatility conditional on a change in the spot

$$\frac{\partial C}{\partial \sigma}\,\mathbb{E}\left[\delta\sigma|\delta S\right].$$

Estimating $\mathbb{E}\left[\delta\sigma(T)|\delta X\right]$

- ATM implied volatilities $\sigma_t(T) = \sigma_{\text{BS},t}(0,T)$ and stock prices are both observable.
- Market makers can estimate the second component using a simple regression:

$$\delta\sigma_t(T) = \beta_t(T)\,\frac{\delta S_t}{S_t} + \text{noise} =: \beta_t(T)\,\delta X_t + \text{noise}.$$

- Then

$$\beta_t(T) = \frac{\mathbb{E}_t\left[d\left\langle \sigma(T), X\right\rangle_t\right]}{\mathbb{E}_t\left[d\left\langle X\right\rangle_t\right]}.$$

The skew-stickiness ratio

- For a given time to expiration T, we define the ATM volatility skew

$$\mathcal{S}_t(T) = \frac{\partial}{\partial k}\sigma_{\rm BS}(k, T)\bigg|_{k=0}.$$

- Bergomi [Ber09, Ber16] calls

$$\mathcal{R}_t(T) = \frac{\beta_t(T)}{\mathcal{S}_t(T)}$$

the *skew-stickiness ratio* or *SSR*.

The quadratic rough Heston model

The quadratic rough (QR) Heston model of [GJR20] may be written as

$$\begin{aligned} \frac{dS_t}{S_t} &= -\sqrt{V_t}\, dW_t, \\ V_t &= Y_t^2 + c, \end{aligned} \tag{1}$$

where the minimum variance $c \geq 0$, and

$$Y_t = \bar{Y} + \int_{-\infty}^{t} \kappa(t-s)\, \sqrt{V_s}\, dW_s = \bar{Y} - \int_{-\infty}^{t} \kappa(t-s)\, \frac{dS_s}{S_s} \tag{2}$$

is a weighted average of historical returns and $\kappa(\cdot)$ a kernel function.

Then, for $u > t$,

$$Y_u = y_t(u) + \int_t^u \kappa(u-s)\,\sqrt{V_s}\,dW_s \tag{3}$$

where

$$y_t(u) := \mathbb{E}_t\left[Y_u\right] = \bar{Y} + \int_{-\infty}^t \kappa(u-s)\,\sqrt{V_s}\,dW_s.$$

Then, $y_\cdot(u)$ is a martingale and

$$dy_t(u) = \kappa(u-t)\,\sqrt{V_t}\,dW_t. \tag{4}$$

Variance of Y_u

Thus $\mathbb{E}_t\left[Y_u\right] = y_t(u)$ and from (4) and Itô's isometry,

$$\mathrm{var}_t[Y_u] = \int_t^u \xi_t(s)\,\kappa(u-s)^2\,ds, \tag{5}$$

where $\xi_t(s) := \mathbb{E}_t\left[V_s\right]$ for all $s \geq t$.

- Under QR Heston, we have the mean and variance of Y_u in (quasi-) closed form.

Remark

The QR Heston model with $c = 0$ and kernel $\kappa(\tau) = \nu\, e^{-\lambda\tau}$ is an inverse gamma model with $\rho = -1$.

The forward variance curve

From the model definition (1), for $u > t$, $V_u = y_u(u)^2 + c$ so applying Itô's Formula, we have

$$\begin{aligned} \xi_t(u) &= \mathbb{E}_t\left[y_u(u)^2\right] + c \\ &= y_t(u)^2 + \mathbb{E}_t\left[\int_t^u d\left\langle y_\cdot(u)\right\rangle_s\right] + c \\ &= y_t(u)^2 + \int_t^u \xi_t(s)\,\kappa(u-s)^2\,ds + c. \end{aligned} \tag{6}$$

Alternatively,

$$y_t(u)^2 = \xi_t(u) - \int_t^u \xi_t(s)\,\kappa(u-s)^2\,ds - c, \tag{7}$$

- $y_t(u)$ may be easily imputed from the forward variance curve.

$\xi_t(u)$ from $y_t(u)$

(6) is a Wiener–Hopf equation for $\xi_t(u)$ whose solution may be written as

$$\xi_t(u) = y_t(u)^2 + c + \int_t^u K(u-s)\,\left[y_t(s)^2 + c\right]\,ds. \tag{8}$$

- The Laplace transform (denoted as $\mathcal{L}$) of the resolvent kernel K is given by

$$\mathcal{L}[K] = \frac{\mathcal{L}[\kappa^2]}{1-\mathcal{L}[\kappa^2]}. \tag{9}$$

  - Note that for this to make sense, we must have

$$\|\kappa^2\| = \mathcal{L}[\kappa^2](0) < 1.$$

The stationary state

- In the stationary state, $\mathbb{E}\left[Y_t\right] = \bar{Y}$ and

$$\begin{aligned}\bar{V} := \mathbb{E}\left[V_t\right] = \mathbb{E}\left[c + Y_t^2\right] \\ &= c + \bar{Y}^2 + \int_{-\infty}^{t} \kappa(t-s)^2\, \mathbb{E}\left[V_s\right] ds \\ &= c + \bar{Y}^2 + \left\|\kappa^2\right\| \bar{V}, \qquad (10)\end{aligned}$$

where $\left\|\kappa^2\right\| = \int_0^\infty \kappa(s)^2\, ds$.

- It follows again that we must have

$$\left\|\kappa^2\right\| < 1.$$

  - Violated by the power-law kernel!

Dynamics of forward variance

Applying Itô's Formula to (8) and using that $\xi_\cdot(u)$ is a martingale,

$$
\begin{aligned}
d\xi_t(u) &= 2\, y_t(u)\, dy_t(u) + 2 \int_t^u y_t(s)\, dy_t(s)\, K(u-s)\, ds \\
&= 2 \left\{ y_t(u)\, \kappa(u-t) + \int_t^u y_t(s)\, \kappa(s-t)\, K(u-s)\, ds \right\} \sqrt{V_t}\, dW_t \\
&= -2 \left\{ \kappa(u-t)\, y_t(u) + \int_t^u \kappa(s-t)\, K(u-s)\, y_t(s)\, ds \right\} \frac{dS_t}{S_t}.
\end{aligned}
\tag{11}
$$

Choice of kernel

- We choose the gamma kernel.

$$\kappa(\tau) = \frac{\nu}{\Gamma(\alpha)}\, \tau^{\alpha-1}\, e^{-\lambda\,\tau}. \tag{12}$$

  - With this choice, the QR Heston model has only four parameters: H, ν, λ, and c.

- There is a closed-form expression for the resolvent kernel:

$$K(\tau) = \hat{\nu}^2\, e^{-2\lambda\tau}\, \tau^{2H-1}\, E_{2H,2H}(\hat{\nu}^2\, \tau^{2H}),$$

where $E_{\bullet,\bullet}$ is the two-parameter Mittag–Leffler function.

The QRH simulation scheme

- Recall the dynamics of $y_\bullet(u)$ from (4):

$$dy_t(u) = \kappa(u-t)\sqrt{V_t}\,dW_t.$$

- The dynamics of y are formally identical to those of ξ in an affine forward variance (AFV) model.
  - Thus, we may use the HQE scheme of [Gat22] to simulate y.

Simulating Y

- Following [Gat22] closely, we have from (3) that

$$Y_T = y_T(T) = y_t(T) + \int_t^T \kappa(T-s)\,\sqrt{V_s}\,dW_s. \tag{13}$$

- Wlog, let $t = 0$.Then, with more-or-less obvious notation,

$$Y_n = y_n + \sum_{k=1}^{n} \int_{(k-1)\Delta}^{k\Delta} \kappa(n\Delta - s)\,\sqrt{V_s}\,dW_s =: \hat{y}_n + u_n,$$

  - The $\mathcal{F}_{n-1}$-adapted variable $\hat{y}_n$ is given by

$$\hat{y}_n := \mathbb{E}\left[\,Y_n \middle|\, \mathcal{F}_{n-1}\right] = y_n + \sum_{k=1}^{n-1} \int_{(k-1)\Delta}^{k\Delta} \kappa(n\Delta - s)\,\sqrt{V_s}\,dW_s,$$

  - The martingale increment u_n is given by

$$u_n := \int_{(n-1)\Delta}^{n\Delta} \kappa(n\Delta - s)\,\sqrt{V_s}\,dW_s.$$

The X-process

- We also need to simulate the nth increment of the component of the log-stock price process $X = \log S$:

$$\chi_n := \int_{(n-1)\Delta}^{n\Delta} \sqrt{V_s}\, dW_s.$$

Notation

- Now define for every $i, j \in \mathbb{N}$,

$$\mathcal{K}_i(\Delta) := \int_0^\Delta \kappa(s + i\Delta)\, ds$$
$$\mathcal{K}_{i,j}(\Delta) := \int_0^\Delta \kappa(s + i\Delta)\kappa(s + j\Delta)\, ds.$$

  - For the gamma kernel (12),

$$\mathcal{K}_i(\Delta) = \frac{\nu}{\lambda^{H+1/2}\Gamma(\alpha)} \left[\Gamma(H + 1/2, i\lambda\Delta) - \Gamma(H + 1/2, (i + 1)\lambda\Delta)\right],$$
$$\mathcal{K}_{i,i}(\Delta) = \frac{\nu^2}{(2\lambda)^{2H}\Gamma(\alpha)^2} \left[\Gamma(2H, 2i\lambda\Delta) - \Gamma(2H, 2(i + 1)\lambda\Delta)\right],$$

where $\Gamma(s, x) = \int_x^\infty t^{s-1} e^{-t}\, dt$.

Computation of $\mathrm{var}\left[\, u_n \middle| \, \mathcal{F}_{n-1} \right]$

The conditional variance may be approximated by

$$\begin{aligned} \mathrm{var}\left[\, u_n \middle| \, \mathcal{F}_{n-1} \right] &= \mathrm{var}\left[\, Y_n \middle| \, \mathcal{F}_{n-1} \right] \\ &\approx \left[\theta \, \hat{y}_n^2 + (1-\theta)\, Y_{n-1}^2 + c\right] \, K_0(\Delta) \\ &=: \bar{V}_n \, \mathcal{K}_{0,0}(\Delta), \end{aligned}$$

with $\theta := \frac{1}{2H+1}$ and

$$K_0(\Delta) := \int_0^{\Delta} K(s)\, ds, \tag{14}$$

where K is the resolvent kernel of κ^2, see (9).

Simulation of u_n and χ_n

- As in [Gat22], we make the hybrid approximation $u_n \approx \beta_{u\chi}\,\chi_n + \varepsilon_n$, where $\beta_{u\chi} = \mathcal{K}_0(\Delta)/\Delta$.
- We simulate χ_n and ϵ_n as

$$\chi_n \sim \sigma_\chi\, Z_\chi; \quad \epsilon_n \sim \sigma_\epsilon\, Z_\epsilon,$$

where Z_χ and Z_ϵ are two independent standard normal random variables, and

$$\sigma_\chi^2 = \bar{V}_n\,\Delta; \quad \sigma_\epsilon^2 = \bar{V}_n\,\left[\mathcal{K}_{0,0}(\Delta) - \mathcal{K}_0(\Delta)^2/\Delta\right],$$

  - In the large n limit, $\mathrm{var}[u_n]$, $\mathrm{var}[\chi_n]$ and $\mathrm{cov}[u_n\,\chi_n]$ are matched.

Simulation of $\hat{y}_n$

- For any $j \in \mathbb{N}^*$, let $b_j^\star$ be the root mean square average of the kernel κ over the jth interval[1]:

$$b_j^\star = \sqrt{\frac{1}{\Delta} \int_{(j-1)\Delta}^{j\Delta} \kappa^2(s)\, ds} = \sqrt{\frac{1}{\Delta} \mathcal{K}_{j-1,j-1}(\Delta)}.$$

- At the nth step of the algorithm, we need $\hat{y}_n = \mathbb{E}\left[y_n \middle| \mathcal{F}_{n-1} \right]$:

$$\hat{y}_n \approx y_n + \sum_{k=1}^{n-1} b_{n-k+1}^\star \, \chi_k .$$

  - Note the explicit path-dependence!

[1]This choice ensures that quadratic variations are matched exactly.

Simulation of V_n and X_n

Having now simulated $\hat{y}_n$ and u_n, we simulate V_n and $X_n = \log(S_n)$ as

$$V_n = Y_n^2 + c = (\hat{y}_n + u_n)^2 + c,$$
$$X_n = X_{n-1} - \tfrac{1}{4}\left(V_n + V_{n-1}\right)\Delta - \chi_n.$$

Remark

At this point, we have simulated X and its quadratic variation, so we can, in principle, price all SPX derivatives, including variance swaps.

SPX option valuation

To be even more explicit, we value a European call expiring at time T as

$$\begin{aligned}\mathbb{E}\left[(S_T - K)^+\right] &= \mathbb{E}\left[\left(S_0\, e^{X_T} - K\right)^+\right] \\ &\approx \frac{1}{M}\sum_{j=1}^{M}\left(S_0 \exp\left\{X_{N,j}\right\} - K\right)^+,\end{aligned}$$

where

- M is the number of Monte Carlo paths,
- $N = T/\Delta$ is the number of time steps.

Simulation of VIX

- Let $\delta = 30/365$ (30 days).
- Given $y_T(u)$, $u > T$, we can show that, under quadratic rough Heston,

$$\mathrm{VIX}_{\mathrm{T}}^2 = \frac{1}{\delta} \int_0^{\delta} \left(y_T(T+u)^2 + c\right) \{1 + K_0(\delta - u)\} \, du, \quad (15)$$

where $K_0(\tau) = \int_0^{\tau} K(s)\, ds$.

Simulation of the $y_T(u)$

- For any $u > T$,

$$
\begin{aligned}
y_T(u) &= y(u) + \int_0^T \kappa(u-s)\,\sqrt{V_s}\,dW_s \\
&\approx y(u) + \sum_{k=1}^{m} a_k(u) \int_{(k-1)\Delta}^{k\Delta} \sqrt{V_s}\; dW_s \\
&= y(u) + \sum_{k=1}^{m} a_k(u)\,\chi_k,
\end{aligned}
$$

where the $a_k(u)$ are chosen so as to match the variances of the $y_T(u)$.

Final VIX simulation recipe

- Plugging into (15) gives

$$\begin{aligned}\mathrm{VIX}_T^2 &= \frac{1}{\delta}\int_0^\delta \left(y_T(T+u)^2 + c\right)\left(1 + K_0(\delta - u)\right)\,du \\ &= \frac{1}{\delta}\int_0^\delta \left[\left(y(T+u) + \sum_{k=1}^n a_k(T+u)\,\chi_k\right)^2 + c\right] \\ &\qquad \times \left[1 + K_0(\delta - u)\right]\,du.\end{aligned}$$

- A numerical integral that may be easily computed.
  - For example, using the trapezoidal rule or a Gauss–Legendre quadrature.

Options on VIX: An example

- We consider a 1 month option on VIX.
- We use parameters from the 15-February 2023 calibration.
- We select 5 Monte Carlo paths and plot the forward variance curves as of time $T = 1m$ corresponding to these paths.
- Recall that

$$VIX_T^2 = \frac{1}{\delta} \int_T^{T+\delta} \xi_T(u)\, du.$$

  - Valuation depends on the forward variance curve between $T = 1m$ and $T = 2m$.
  - We show this graphically in Figure 1.

Options on VIX: Graphical illustration

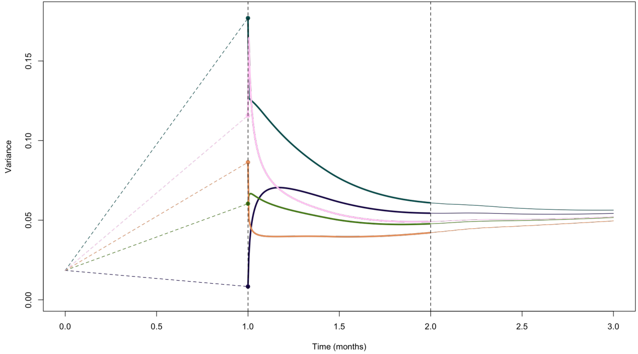

Figure 1: Five forward variance curves contributing to the valuation of a 1-month option on VIX.

Path-dependence of the QR Heston model

- From (11), changes in the forward variance curve are directly expressible in terms of changes in the underlying.
  - The QR Heston model is thus purely path-dependent.
- Explicitly, using $dy_t(u) = \kappa(u-t)\sqrt{V_t}\,dW_t$, we may write

$$y_t(u) = \bar{Y} + \int_{-\infty}^{t} \kappa(u-r)\sqrt{V_r}\,dW_r = \bar{Y} - \int_{-\infty}^{t} \kappa(u-r)\,\frac{dS_r}{S_r}.$$

  - The forward volatility curve is thus a weighted average of historical stock returns.
- The fair values of SPX options, VIX options, and the SSR are all functionals of the forward volatility curve.

Examples of path-dependence

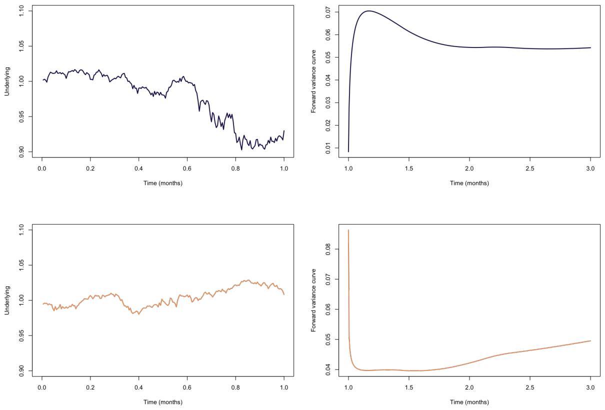

Figure 2: Two price paths and corresponding forward variance curves. With our fitted parameters, the forward variance curve is most sensitive to the very recent past.

Estimation of the SSR

- Recall that the SSR is given by

$$\mathcal{R}_t(T) = \frac{\beta_t(T)}{\mathcal{S}_t(T)}$$

where

- $\beta_t(T)$ is the regression coefficient in

$$\delta\sigma_t(T) = \beta_t(T)\,\delta X_t + \text{noise},$$

- and $\mathcal{S}_t(T)$ is the ATM skew.

Estimation of the regression coefficient $\beta_t(T)$

- Recall that the QR Heston model reads:

$$dy_t(u) = \kappa(u-t)\sqrt{V_t}\, dW_t.$$

- We apply the finite difference methodology of Bourgey et al. [BDDM24].
- Thus, the regression coefficient is estimated as

$$\beta_t(T) \approx \frac{1}{h}\left\{\sigma_t\left(T, y_t^h(\cdot)\right) - \sigma_t\left(T, y_t(\cdot)\right)\right\},$$

where h is a small parameter, and for $t \leq u \leq T$,

$$y_t^h(u) := y_t(u) - h\,\kappa(u-t). \tag{16}$$

Estimation of the ATM skew $\mathcal{S}_t(T)$

- Recall that the ATM skew

$$\mathcal{S}_t(T) = \left.\frac{\partial \sigma_{\mathrm{BS}}(k,T)}{\partial k}\right|_{k=0}.$$

- We estimate the ATM skew using a trick from [BDMFP23].
-

$$\frac{\partial \sigma_{\mathrm{BS}}(k,T)}{\partial k} = \left.\frac{\Phi\left(-\frac{k}{\sqrt{w}} - \frac{\sqrt{w}}{2}\right) - \mathbb{P}(X_T \geq k)}{\sqrt{T}\phi\left(-\frac{k}{\sqrt{w}} - \frac{\sqrt{w}}{2}\right)}\right|_{w=T\sigma^2_{\mathrm{BS}}(k,T)}$$

where $X_T = \log(\frac{S_T}{S_0})$ and ϕ is the p.d.f. of a standard normal distribution.

Estimation of the SSR

- Finally, the SSR is estimated as

$$\mathcal{R}_t(T) \approx \frac{\beta_t(T)}{\mathcal{S}_t(T)}. \qquad (17)$$

Remark

The estimator (17) only requires only the ATM implied volatilities for two different forward volatility curves $y_t(u)$, and one estimate of the ATM skew.

Calibrated parameters

- As reference dates, we choose 19 December 2024, 16 April 2025, 20 June 2025, and 2 July 2025[2].
  - In Figure 3 we see that these dates span quite distinct market environments.
- Calibrated parameters were

Date	H	ν	λ	c
20241219	0.0964	0.7620	6.256	4.557×10^{-3}
20250416	0.2908	1.2942	5.000	18.977×10^{-3}
20250620	0.0233	0.3676	6.398	2.308×10^{-3}
20250702	0.0242	0.3669	5.640	2.816×10^{-3}

Table 1: Calibrated parameters for the QRH model.

[2] Closing prices of SPX and VIX options from Cboe DataShop https://datashop.cboe.com.

Forward variance curves

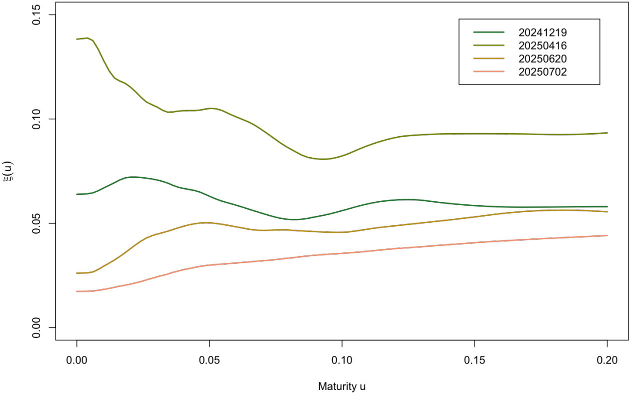

Figure 3: Plots of the forward variance curves for each reference date.

Some SPX smiles as of 20 June 2025

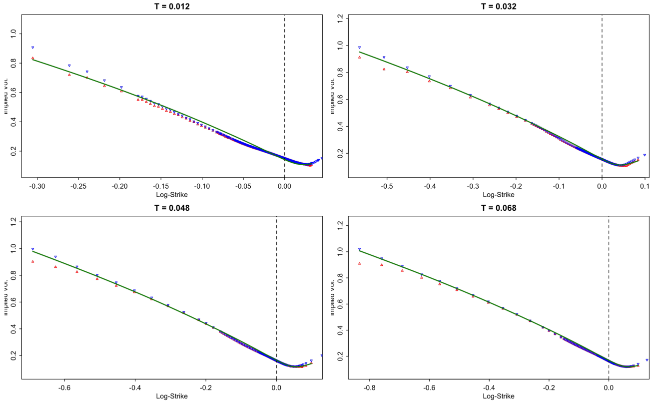

Figure 4: SPX smiles as of 20 June 2025. Bid and offer implied volatilities are in red and blue respectively; green lines are QR Heston fits.

Some VIX smiles as of 20 June 2025

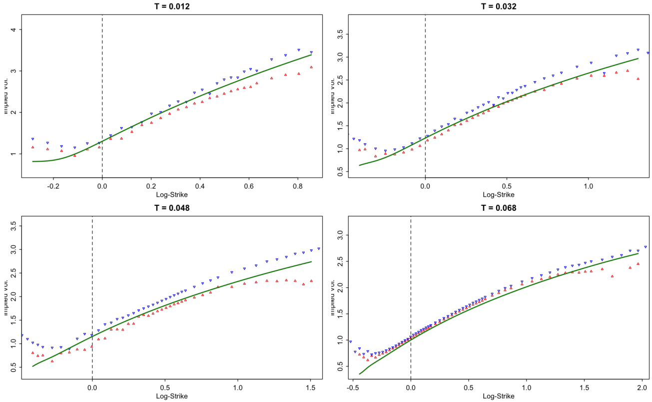

Figure 5: VIX smiles as of 20 June 2025. Bid and offer implied volatilities are in red and blue respectively; green lines are QR Heston fits.

SSR term structures

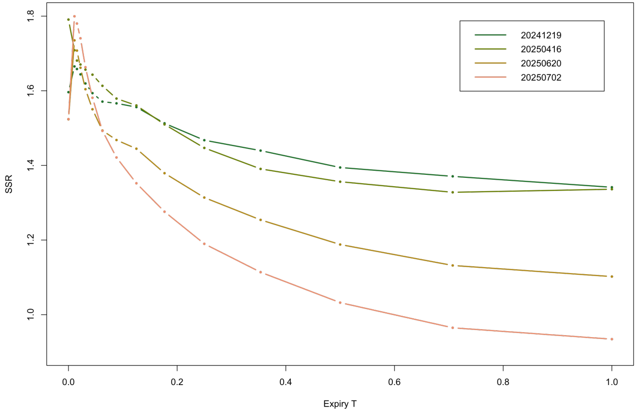

Figure 6: QRH-model SSR term structures for the reference dates.

The time series of SSR from Vola Dynamics

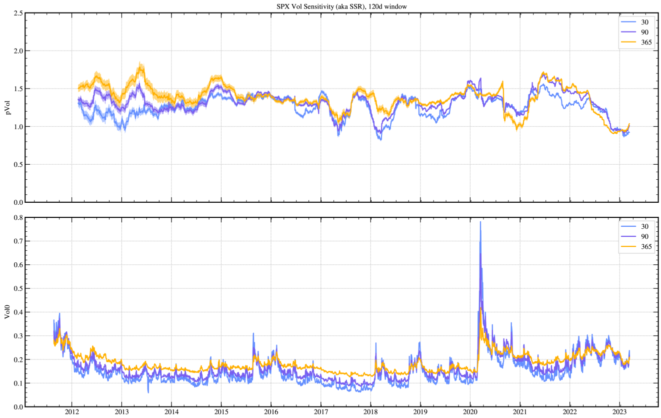

Figure 7: The 30 day, 90 day, and 1 year skew-stickiness ratios (SSR), with a trailing window of 120 days from Vola Dynamics.

Model and observed intraday SSRs

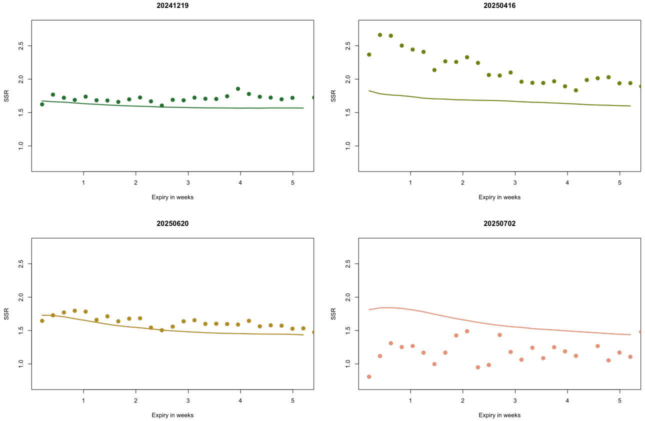

Figure 8: VIX smiles as of 20 June 2025. Lines are QRH model SSRs; dots are empirical SSRs from 1-minute intraday CBOE data.

Remarks on the fits

- Despite the impressive joint fits to short-dated SPX and VIX smiles, fits deteriorate for longer periods.
- The very short-time behavior of the SSR shown in Figure 6, where the SSR increases sharply before declining, is consistent with the general results derived in [FG24].
  - Model SSR is not always quantitatively consistent with intraday estimates of the SSR.
- $c > 0$ is really necessary.
  - Fits with $c = 0$ are much less impressive.
- Calibrated c increases with vol. and there is a persistent misfit in the extreme left wing of the VIX smile.
  - These point to the need for additional flexibility.

Why does the QR Heston model fit so well?

- In view of its extreme parsimony, it may at first seem surprising that the QR Heston model can generate such impressive fits.
- By taking a historical perspective and relating the QR Heston model to earlier models, we may begin to understand its strong fitting performance.

QR Heston from Quadratic Hawkes

- The QR Heston model in (1) is a special case of the quadratic rough Heston model of [DJR21].
- This model, in turn, emerges as the continuous-time limit of a non-Markovian extension of the quadratic Hawkes model originally proposed in [BDB17].
    - Calibration of that model to intraday data yielded very impressive results.
- Thus the QR Heston model can be seen as a non-Markovian extension of a long-standing successful statistical model of financial markets.

Markovian QR Heston

- The QR Heston model can also be seen as the non-Markovian extension of various realistic models in the classical stochastic volatility literature.
- Consider the QR Heston model in the Markovian case ($H = 1/2$) with the gamma kernel (12):

$$\kappa(\tau) = \nu\, e^{-\lambda\, \tau},$$

  and $c = 0$.
- In this case, $\sigma_t = Y_t$ is the instantaneous volatility and (2) may be rewritten as

$$d\sigma_t = -\lambda\, (\sigma_t - \bar{Y})\, dt + \nu\, \sigma_t\, dW_t, \tag{18}$$

QR Heston and the Inverse Gamma model

- (18) are the dynamics of volatility in the Inverse Gamma model of [LLZ16].
- As noted in that paper, the Inverse Gamma model is a special case of various other models that have desirable properties consistent with empirical studies of stocks and their volatilities.
- For example, the Inverse Gamma model has an inverse gamma stable distribution, which was shown to be a good fit to the unconditional distribution of volatility by Bouchaud and Potters [BP03] and Sepp [SK12], amongst others.
  - In fact, this observation was one of the reasons that Sepp chose his particular model dynamics.

QR Heston and the Double Lognormal model

- In terms of $V_t = \sigma_t^2 = Y_t^2$, (18) may be written in the form

$$
\begin{aligned}
dV_t &= -\hat{\lambda}\left(V_t - V_t'\right) dt + 2\,\nu\, V_t\, dW_t, \\
dV_t' &= -\lambda\left(V_t' - \bar{V}'\right) dt + \nu\, V_t'\, dW_t,
\end{aligned}
$$

where

$$
\hat{\lambda} = 2\,\lambda - \nu^2; \qquad V_t' = \frac{2\lambda}{\hat{\lambda}}\,\bar{Y}\,\sigma_t; \qquad \bar{V}' = \frac{2\lambda}{\hat{\lambda}}\,\bar{Y}^2.
$$

- This is a special case of the Double Lognormal (DL) model of [Gat08]
  - DL generates positively sloping VIX smiles.
  - DL parameters are reasonable stable.

Lifting the Double Lognormal model

- Viewing the gamma kernel as an infinite sum of exponential kernels with different characteristic timescales in the spirit of [AJ19], the QR Heston model may be seen as an infinite sum of Double Lognormal models.
- Accordingly, the QR Heston model inherits various properties of the Double Lognormal model such as positively sloped VIX smiles.

Concluding remarks

- The Quadratic Rough Heston (QR) Heston model can successfully capture the joint behavior of SPX and VIX implied volatility smiles, whilst producing realistic values for the the SSR.
- The QR Heston model with the gamma kernel is:
  - Extremely parsimonious with only four parameters.
  - Econometrically motivated.
  - Non-Markovian.
  - Purely path-dependent.
- The QRH scheme is efficient and easy to implement.
  - The QR Heston model is thus a viable candidate for practical trading applications.
    - See also the QRH+ model of [BNPRS26].

GitHub

- Last but not least, we have made R and Python codes plus Jupyter notebooks illustrating their usage available at `https://github.com/jgatheral/QuadraticRoughHeston`.

References

Eduardo Abi Jaber.
Lifting the Heston model.
Quantitative Finance, 19(12):1995–2013, 2019.

Lorenzo Bergomi
Smile dynamics IV.
Risk December, pages 94–100, 2009.

Lorenzo Bergomi.
Stochastic Volatility Modeling.
Chapman and Hall/CRC, 2016.

Pierre Blanc, Jonathan Donier, and Jean-Philippe Bouchaud.
Quadratic Hawkes processes for financial prices.
Quantitative Finance, 17(2):171–188, 2017.

Jean-Philippe Bouchaud and Marc Potters.
Theory of financial risk and derivative pricing: From statistical physics to risk management.
Cambridge University Press, 2003.

Florian Bourgey, Stefano De Marco, Peter K Friz, and Paolo Pigato.
Local volatility under rough volatility.
Mathematical Finance, 33(4):1119–1145, 2023.

Florian Bourgey, Jules Delemotte, and Stefano De Marco.
Smile dynamics and rough volatility.
SSRN:4911186, 2024.

Florian Bourgey and Jim Gatheral.
The SSR under Quadratic Rough Heston.
SSRN:4911186, 2025.

Florian Bourgey, Patrick Noble, Ingi Örn Petursson, Mathieu Rosenbaum and Grégoire Szymanski.
The Quadratic Rough Heston+ Model for Short-Dated Options.
SSRN:6072928, 2026.

Aditi Dandapani, Paul Jusselin, and Mathieu Rosenbaum.
From quadratic Hawkes processes to super-Heston rough volatility models with Zumbach effect.
Quantitative Finance, 21(8):1235–1247, 2021.

Peter Friz and Jim Gatheral.
Computing the SSR.
Quantitative Finance, 25(5) 2025.

Jim Gatheral.
Consistent modeling of SPX and VIX options.
In *Bachelier congress*, volume 37, pages 39–51, 2008.

Jim Gatheral.
Efficient simulation of affine forward variance models.
Risk.net, February, 2022.

Jim Gatheral, Paul Jusselin, and Mathieu Rosenbaum.
The quadratic rough Heston model and the joint S&P 500/VIX smile calibration problem.
Risk.net, May 2020.

Nicolas Langrené, Geoffrey Lee, and Zili Zhu.
Switching to non-affine stochastic volatility: A closed-form expansion for the inverse gamma model.
International Journal of Theoretical and Applied Finance, 19(5):1650031, 2016.

Aitor Muguruza.
Not so Particular about Calibration: Smile Problem Resolved.
arXiv:1909.13366, 2019.

Artur Sepp and Piotr Karasinski.
Beta stochastic volatility model.
Risk Magazine, pages 66–71, October, 2012.